Violet Grove 2D and 3D data processing at CREWES

Han-xing Lu, Kevin Hall, and Don C. Lawton

ABSTRACT

Several north-south and east-west 3C-2D seismic lines were acquired at the Penn West CO_2 pilot project in west-central Alberta in March 2005. The lines were positioned around a monitoring well in the portion of the Pembina Field operated by Penn West Petroleum Ltd. Data were also recorded on a series of permanent 3C geophones in an observation well. These data represent a baseline survey of the reservoir prior to commencement of a CO_2 injection project. CREWES has reprocessed the data in preparation for time-lapse analysis following the first monitor survey, which is scheduled for January 2006.

INTRODUCTION

A series of N-S and E-W 3C-2D seismic lines was acquired by Veritas DGC Inc. in April of 2005. These lines were located in a portion of the Pembina Field operated by Penn West Petroleum Ltd. (Figure 1). Data were simultaneously recorded on a series of permanent 3C geophones in an observation well, as described by Couëslan et al. (2005). These data represent a baseline survey of the reservoir prior to commencement of a CO_2 injection project. The seismic line data will be reacquired in January 2006, for the purposes of a time-lapse study of the CO_2 flood (Lawton et al., 2005).

The surface seismic data have been initially processed as separate 2D lines and as a 3D volume by Veritas DGC, and this version of the 3D volume has been interpreted by Chen and Lawton (2005). Line 1 has also been processed as a 2D line at CREWES, and all five lines have been processed as a 3D volume. These results are presented here.

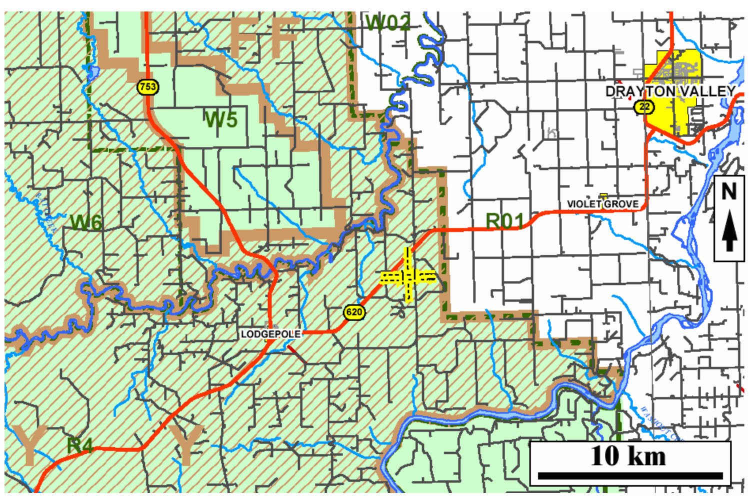

FIG. 1. Location of seismic survey is shown in black dashed lines on a yellow background, centre of map, southwest of Drayton Valley (See Figure 2 for a more detailed survey map).

Acquisition

The Violet Grove survey consists of five 2D lines with a total line length of about 11 km. The data were acquired using single Sercel DSUs (digital seismic units) every 20 m, and dynamite (2 kg at ~15 m depth; Table 1) at a nominal source interval of 40 m. Lines 1-3 are approximately 3 km in length and incorporate both sources and receivers. The line length was chosen to provide a good range of source-receiver offsets at the injection pad, for attribute analysis. The injection zone is ~1640 m below the surface. Lines 4 and 5 are about 0.8 km long, and were receiver lines for the 2005 survey. All receivers were live for all shots. In addition, every shot was recorded by analog 3C geophones permanently cemented in the observation well near the intersection of lines 3 and 5 (Figure 2). In general, the raw data quality is very good.

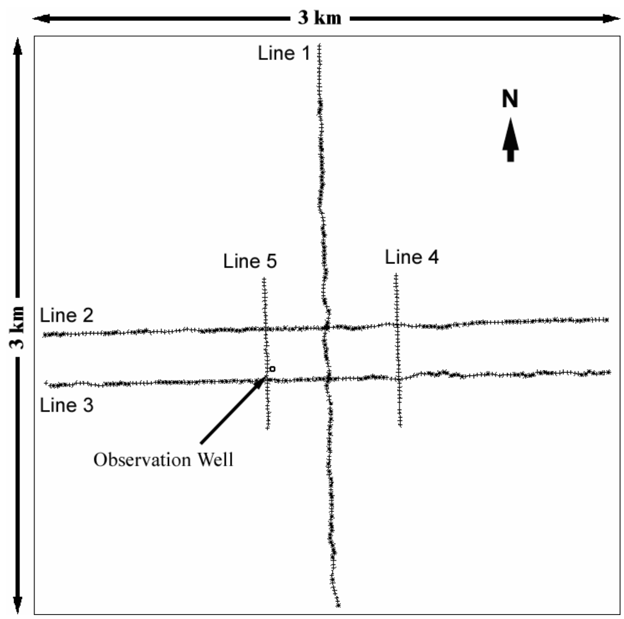

FIG. 2. Survey geometry (modified from ProMAX). Lines 1-3 are 3C-2D seismic lines, Lines 4 and 5 are 3-C receiver lines. Location of the observation well is shown near intersection of lines 3 and 5. All receivers were live for all shots.

Table 1. Acquisition parameters

Source	2 kg dynamite at ~15 m depth
Receiver	Single Sercel DSU
Receiver interval	20 m
Source interval (nominal)	40 m
Maximum source-receiver offset	~3000 m
Record length	4 s
Sample rate	1 ms

3C-2D PROCESSING

The data for line 1 were extracted from the field records, and separated into the vertical (V; Figure 3) and horizontal components (H1 and H2). For radial and transverse component processing (R and T), a component rotation had to be performed, since line 1 has a bearing of 178^{o} from geographic North and the geophones were planted with H1 oriented towards magnetic north. For now, the rotation is purely geometric. Figures 4 and 5 show the horizontal components of source 1141 before (left side) and after rotation (right side). Note that more energy appears on the radial component, especially for longer traveltimes, than can be seen on H1.

Further processing for the vertical, radial and transverse components was performed using standard CREWES processing flows (Table 2). The P-S processing flow is described in greater detail by Lu and Hall (2003). The final migrated vertical, radial and transverse stacks are shown in Figures 6, 7 and 8, respectively. The results from the vertical and radial components indicate that there is little structural relief in this area. While coherent reflections can be seen in the radial component, the energy is quite scattered on the transverse component, indicating that there is very weak (if any) anisotropy along this line.

If the radial component stack is scaled by 1.6 (equivalent to a V_P/V_S of 2.2) and compared to the vertical component stack (Figure 9), the reflections match each other very well. This implies that the results for the vertical and radial components are reliable. However, a comparison of the radial and transverse stacks shows little to no correspondence, as expected (Figure 10).

Table 2. Vertical (left) and radial (right) processing flows modified from Lu and Margrave (1998).

TRACE EDIT TRUE AMPLITUDE RECOVERY SURFACE CONSISTENT DECONVOLUTION TIME VARIANT SPECTRAL WHITENING ELEVATION AND REFRACTION STATIC CORRECTIONS VELOCITY ANALYSIS RESIDUAL SURFACE CONSISTENT STATICS NORMAL MOVEOUT TRIM STATICS FRONT END MUTING CDP STACK TIME VARIANT SPECTRAL WHITENING TRACE EQUALIZATION F-XY DECONVOLUTION 3D PHASE-SHIFT MIGRATION FOR TRACE DISPLAY: TRACE EQUALIZATION BANDPASS FILTER TIME VARIANT SCALING	TRACE EDIT ASYMPTOTIC BINNING SURFACE CONSISTENT DECONVOLUTION TIME VARIANT SPECTRAL WHITENING ELEVATION STATICS APPLY FINAL REFRACTION AND RESIDUAL STATICS FROM P-P CONSTRUCT INITIAL P-SV VELOCITY FROM FINAL P-P VEL. VELOCITY ANALYSIS RECEIVER RESIDUAL STATICS (HAND STATICS) VELOCITY ANALYSIS CONVENTIONAL RESIDUAL STATICS VELOCITY ANALYSIS NORMAL MOVEOUT ACP TRIM STATICS FRONT END MUTING ACP STACK (DEPTH-VARIANT STACK AND DMO STACK) TIME VARIANT SPECTRAL WHITENING TRACE EQUALIZATION F-XY DECONVOLUTION 3D PHASE-SHIFT MIGRATION FOR TRACE DISPLAY: TRACE EQUALIZATION BANDPASS FILTER TIME VARIANT SCALING

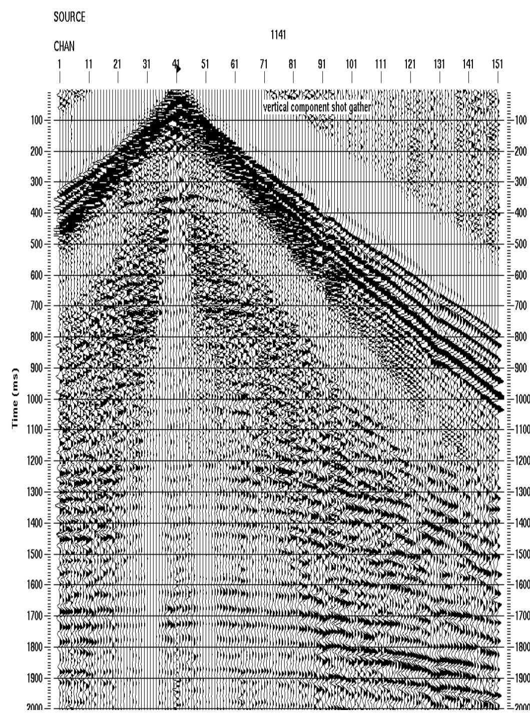

FIG. 3. Raw shot gather for the vertical component of source 1141, for comparison with Figures 4 and 5.

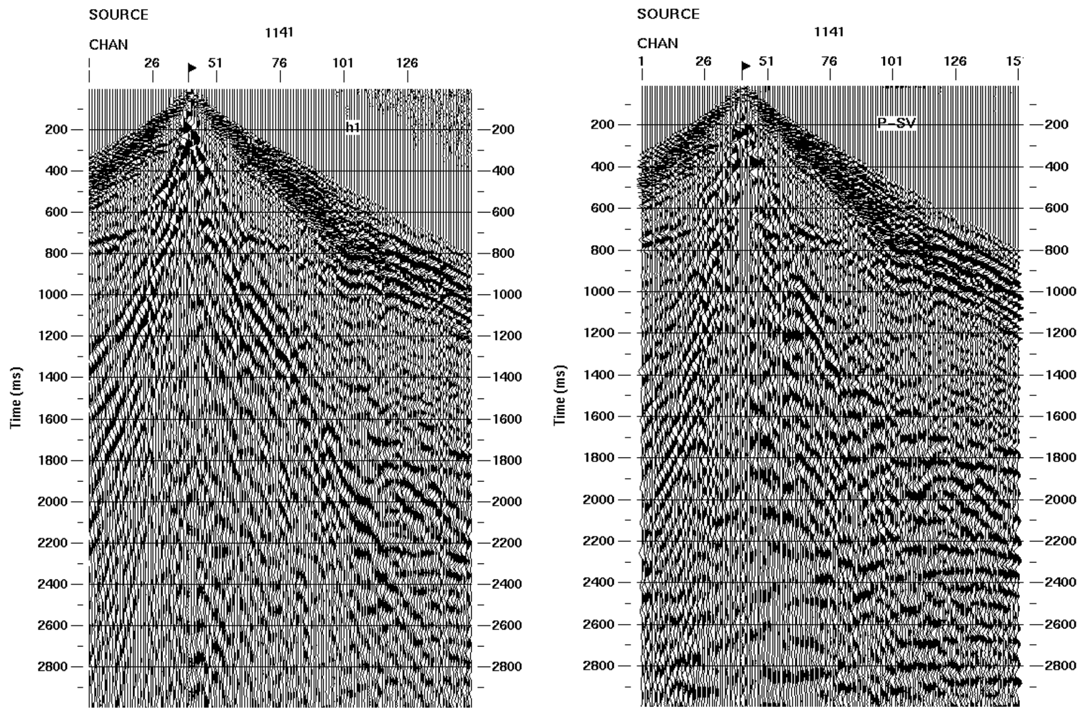

FIG. 4. Raw shot gather for the H1 component (left), and radial component after rotation (right).

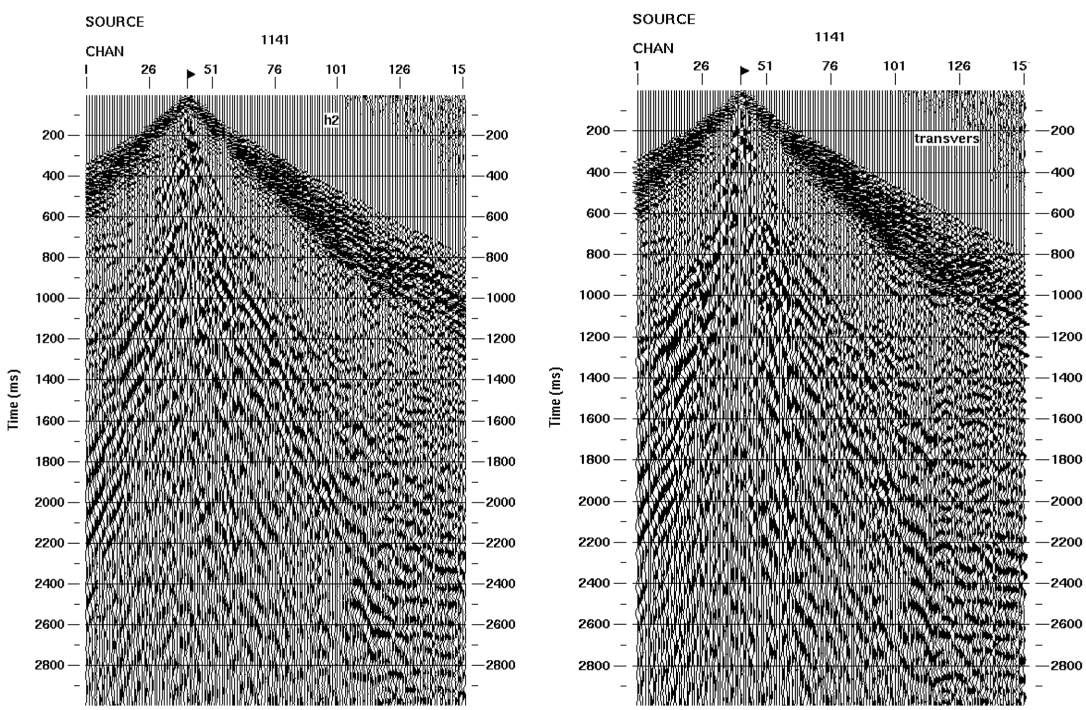

FIG. 5. Raw shot gather for the H2 component (left), and transverse component after rotation (right).

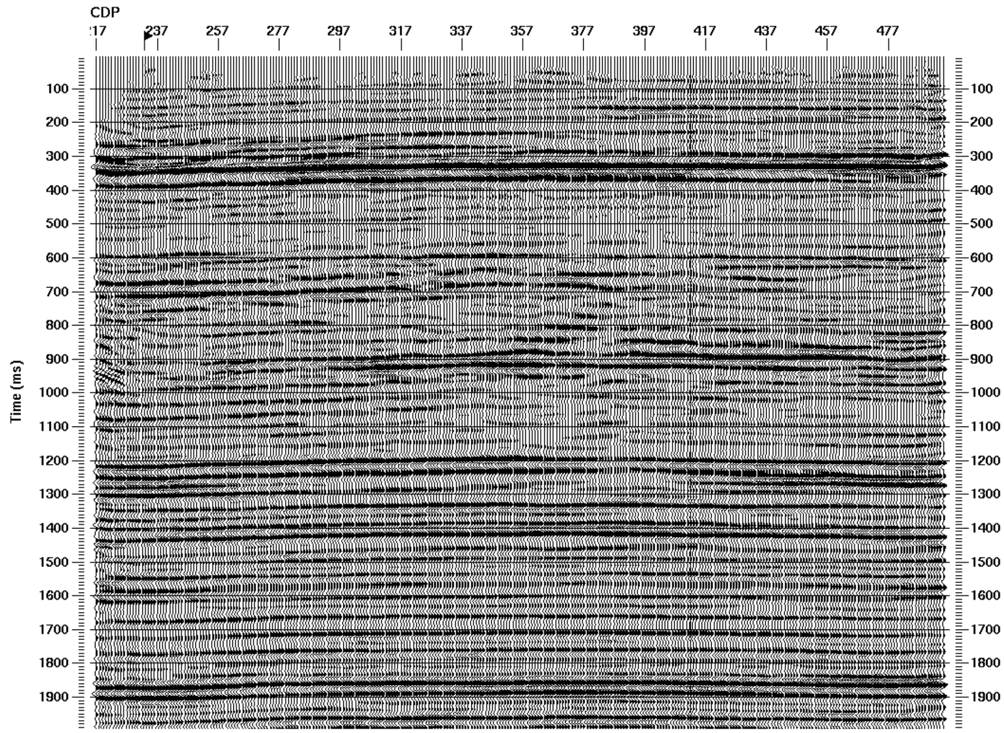

FIG. 6. Time migrated section for the vertical component.

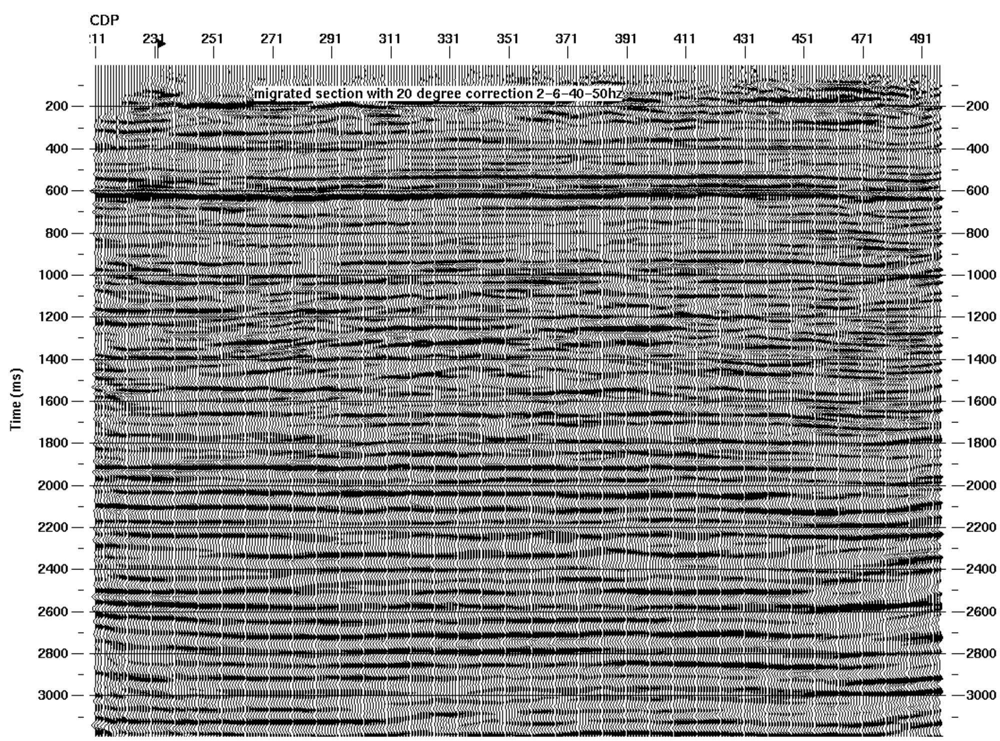

FIG. 7. Time migrated section for the radial component.

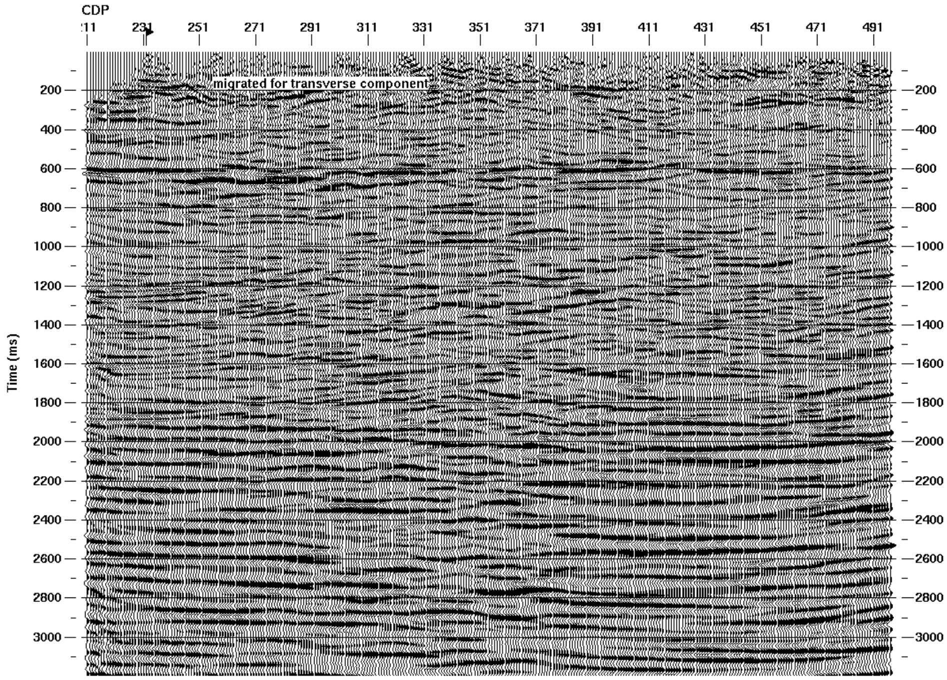

FIG. 8. Time migrated section for the transverse component.

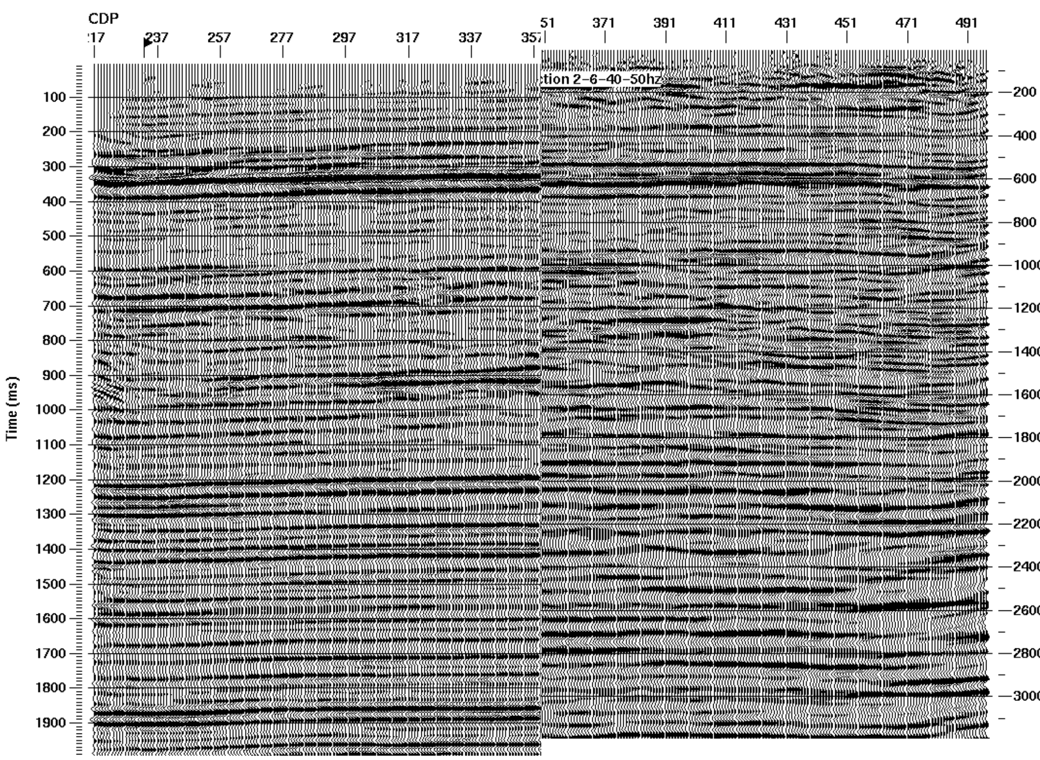

FIG. 9. Comparison of migrated vertical and radial stacks. The radial stack has been stretched to P-P time assuming $V_P/V_S = 2.2$.

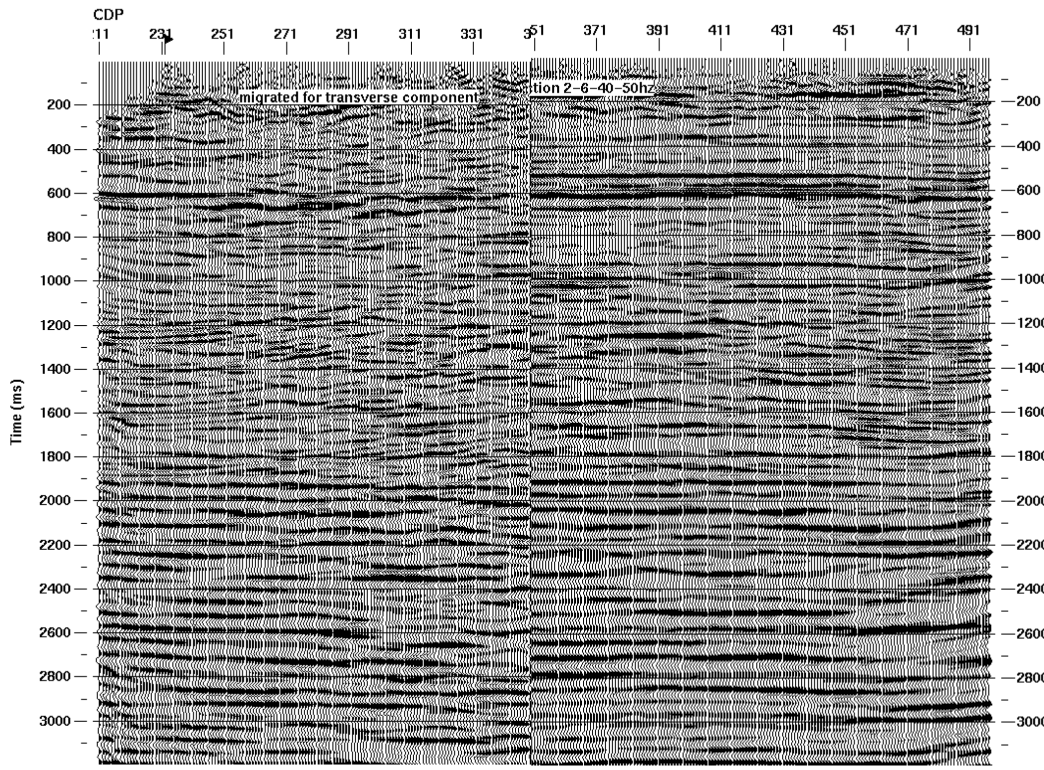

FIG. 10. Comparison of migrated transverse (left) and radial stacks (right).

3C-3D PROCESSING

Due to the design of this survey, CDP and ACP fold tends to be low everywhere except in the middle of the survey. Two different bin sizes have been tested, 20x20 m and 40x40 m, with not much difference (other than spatial resolution) observed in the final results. Only the 20x20 m bin results are presented here (CDP and ACP fold maps are shown in Figures 11 and 12).

Vertical component

The refraction statics results from gli3d clearly show the effect of the survey geometry (Figure 13), but close to the 2D lines, the statics solutions appear to be geologically reasonable (Figure 14). The vertical component was processed using conventional processing, with the following exception; no stretch mute was used after applying NMO corrections (20%-30% stretch mute for NMO is more common). A manually picked top mute was applied post-NMO, in an effort to improve the near-surface coverage of the processed results. Conventional NMO with 20% and 30% stretch mute was also used, and the results in the deeper section are compatible (not shown). Several in-line profiles from the vertical component 3D volume are shown in (Figure 15). The results show good consistent reflections throughout the volume. The 3D result is quite comparable to the 2D result (Figure 16). A series of time slices is also shown (Figure 17).

Radial component

Radial component processing is currently in the receiver statics stage (Figure 18). We hope to complete radial component processing in time to show results at the 2005 CREWES meeting.

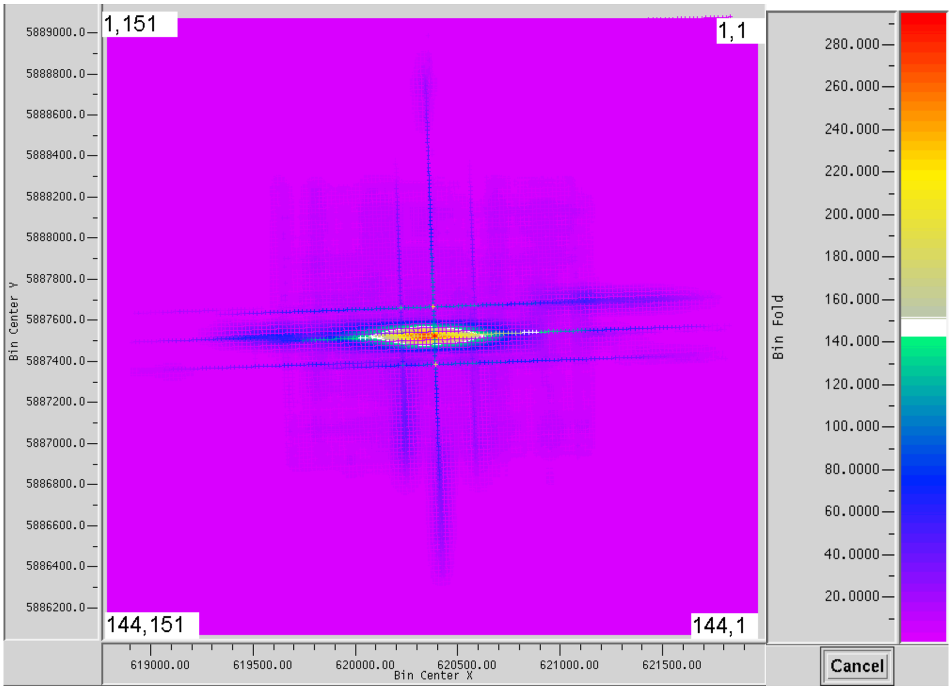

FIG. 11. CDP fold map for the vertical component processed as a 3D with 20x20 m bins. The numbers in the corners denote line numbers (in-line, cross-line).

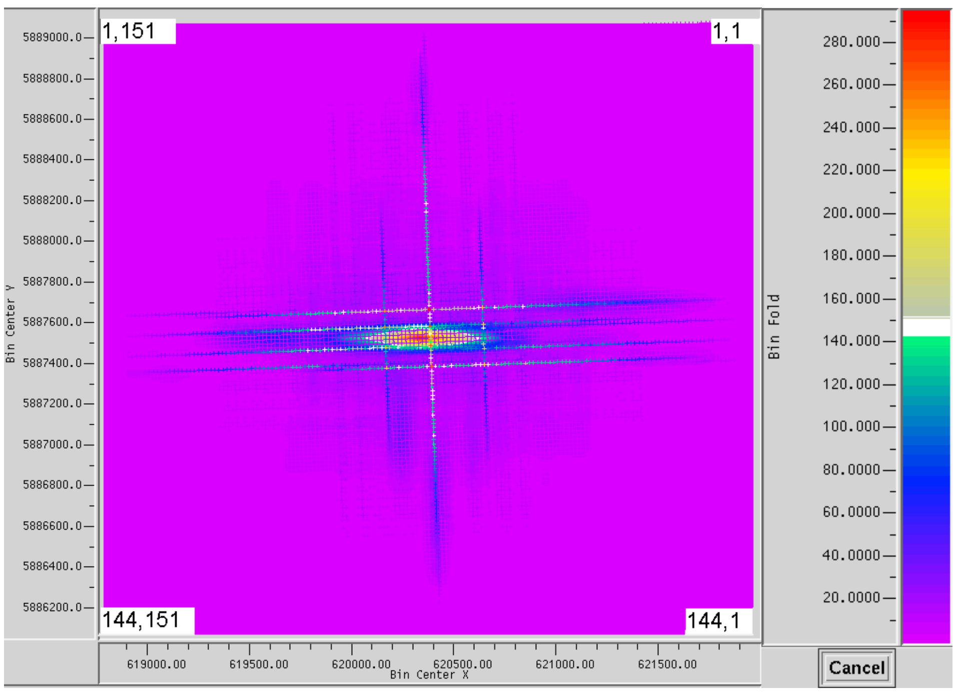

FIG. 12. ACP fold map for the radial component processed as a 3D with 20x20 m bins with an assumed V_P/V_S of 2.2. The numbers in the corners denote line numbers (in-line, cross-line).

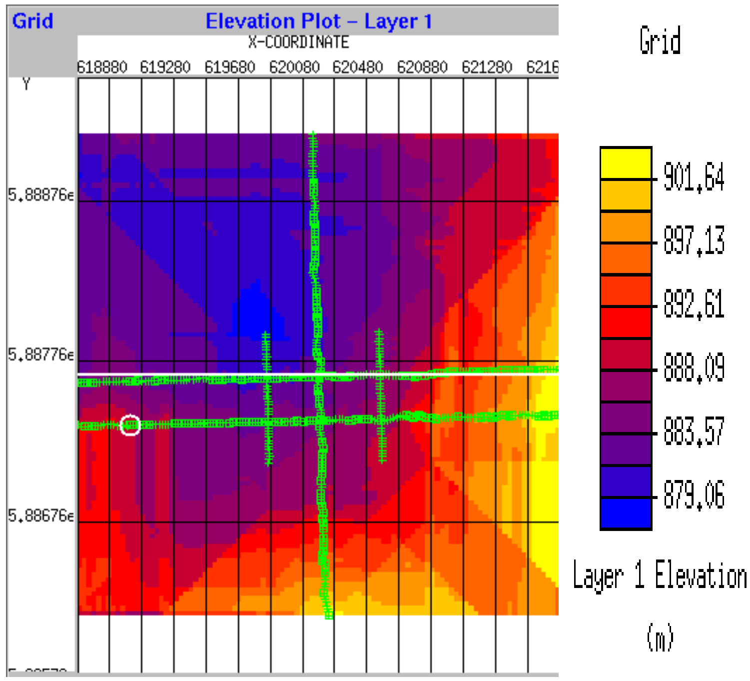

FIG. 13. Modeled elevations for layer one from gli3d. Location of Figure 14 is shown as a white line, roughly coincident with line 2 of the survey (cf. Figure 2).

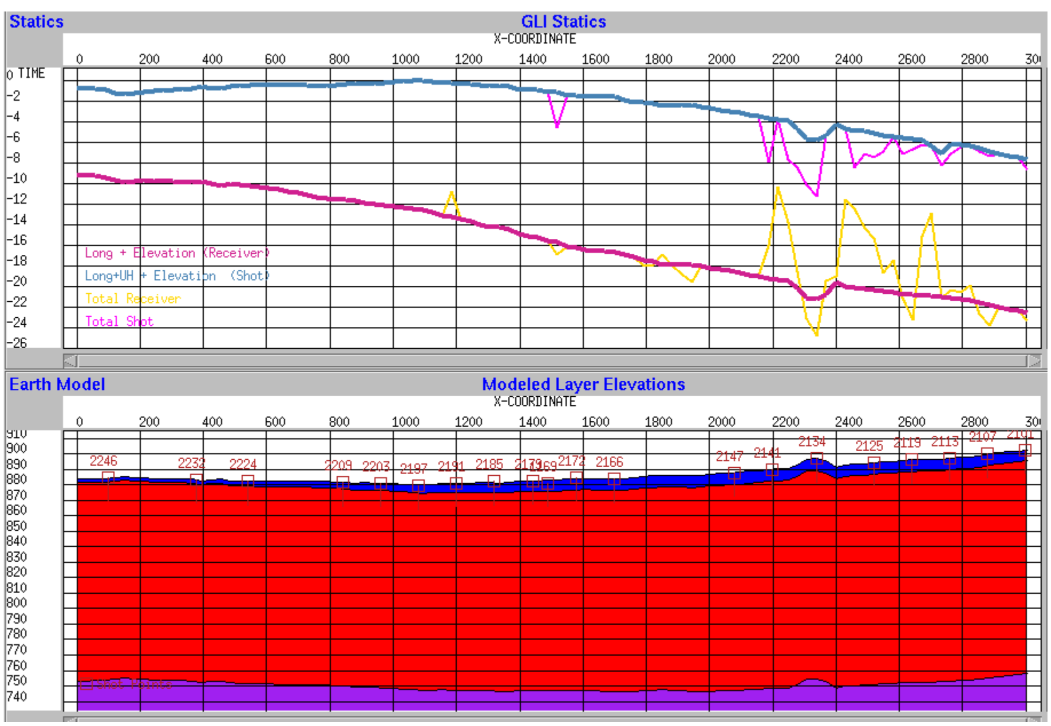

FIG. 14. Total shot statics (pink, top), total receiver refraction statics (yellow, top), and the corresponding velocity model (bottom) calculated with gli3d. Total statics include the elevation, long- and short-wave statics.

a)

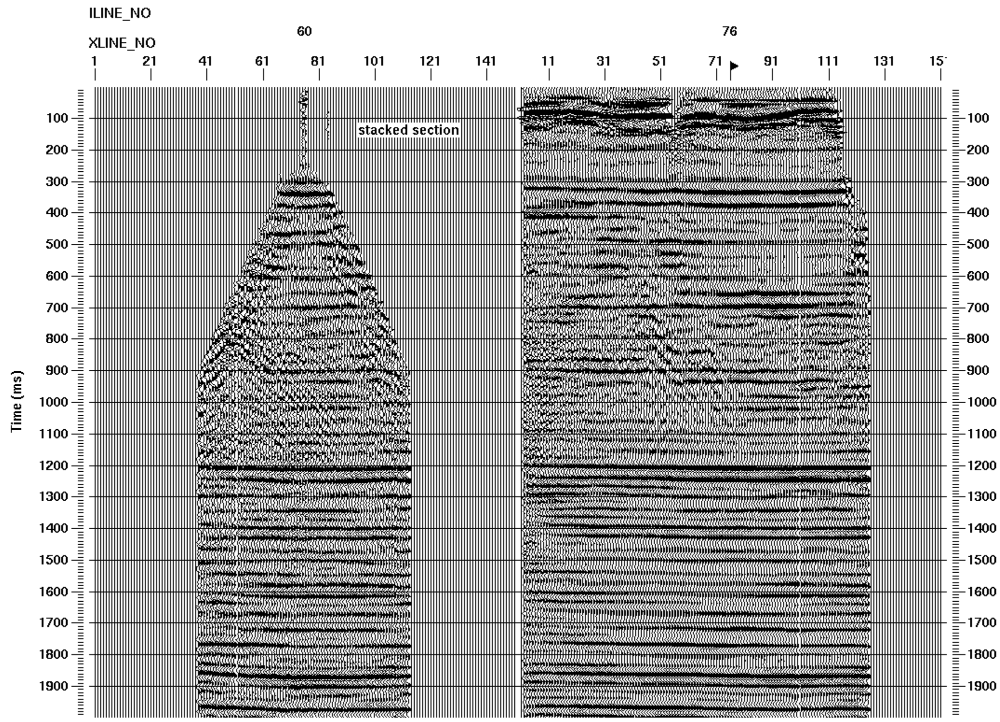
ILINE_NO
60
76
XLINE_NO
1 21 41 61 81 101 121 141 11 31 51 71 91 111 131 15
stacked section
Time (ms)
100 200 300 400 500 600 700 800 900 1000 1100 1200 1300 1400 1500 1600 1700 1800 1900

b)

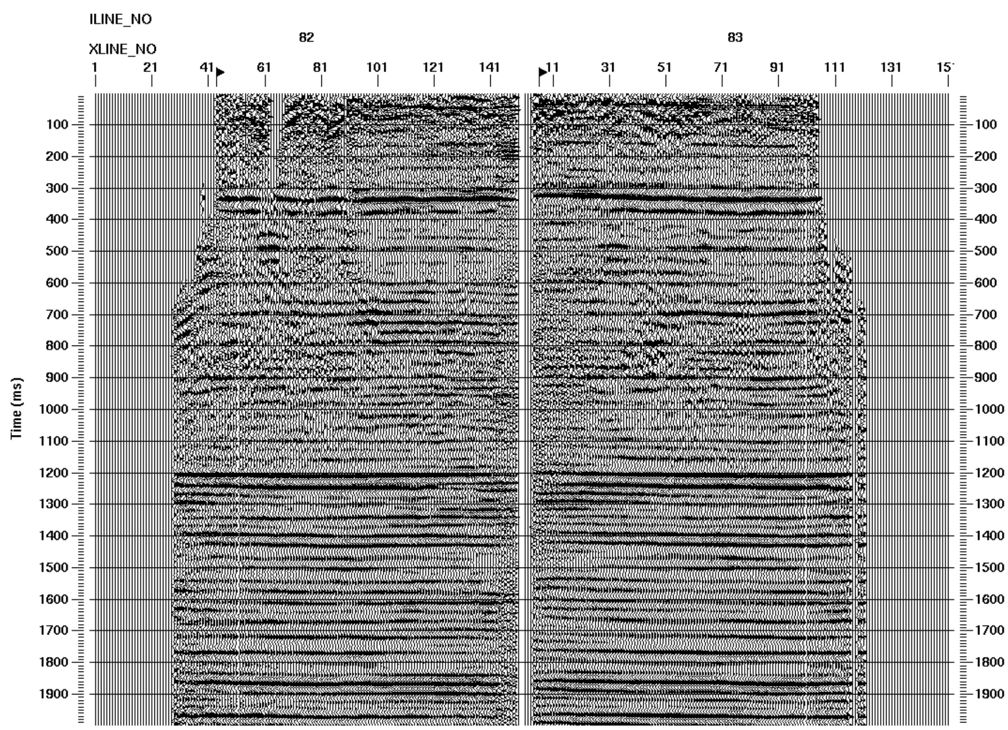
ILINE_NO
82
83
XLINE_NO
1 21 41 61 81 101 121 141 11 31 51 71 91 111 131 15
Time (ms)
100 200 300 400 500 600 700 800 900 1000 1100 1200 1300 1400 1500 1600 1700 1800 1900

c)

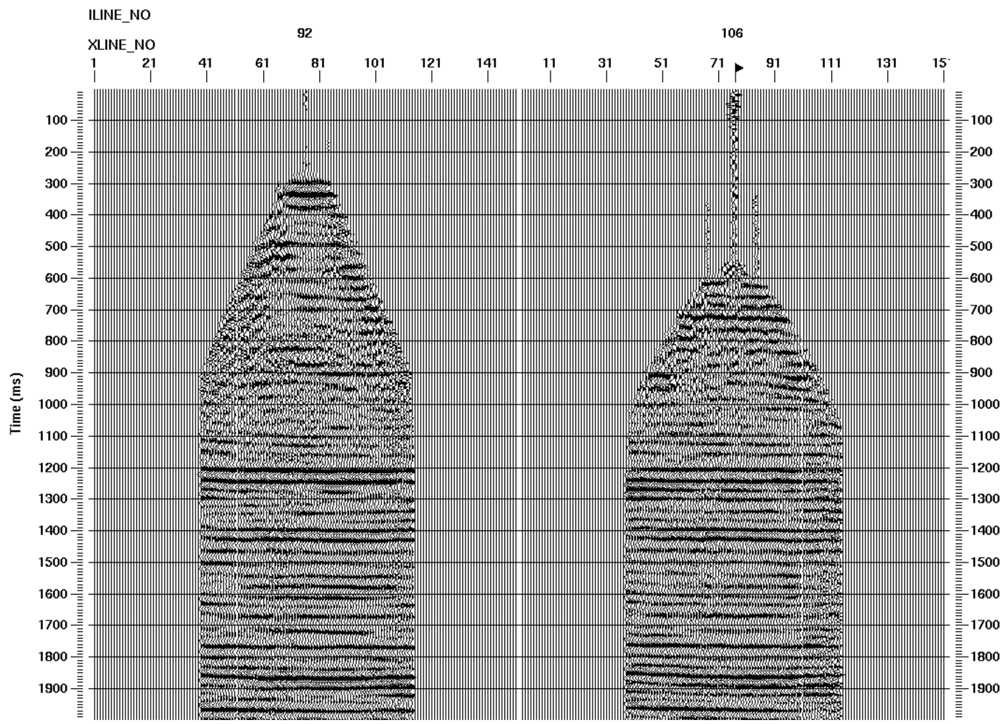

FIG. 15. Comparison of in-lines 60 and 76 (a), 82 and 83 (b), and 92 and 106 (c)

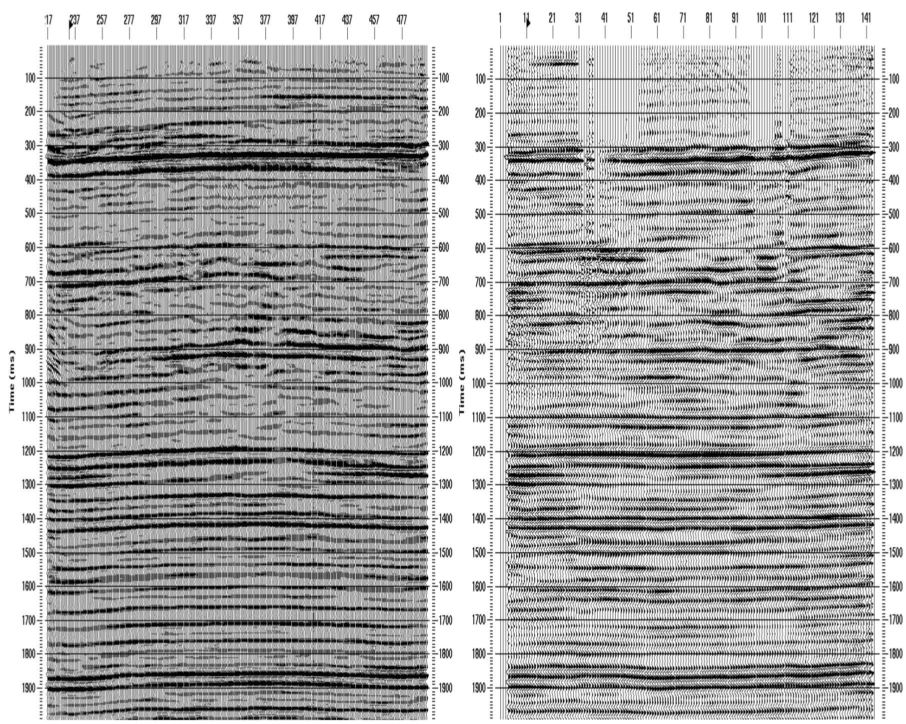

FIG. 16. Comparison of the stacked section for the vertical component of Line 1 processed as a 2D (left) to cross-line 76 (same geographic location as Line 1) of the vertical component 3D volume (right).

a)

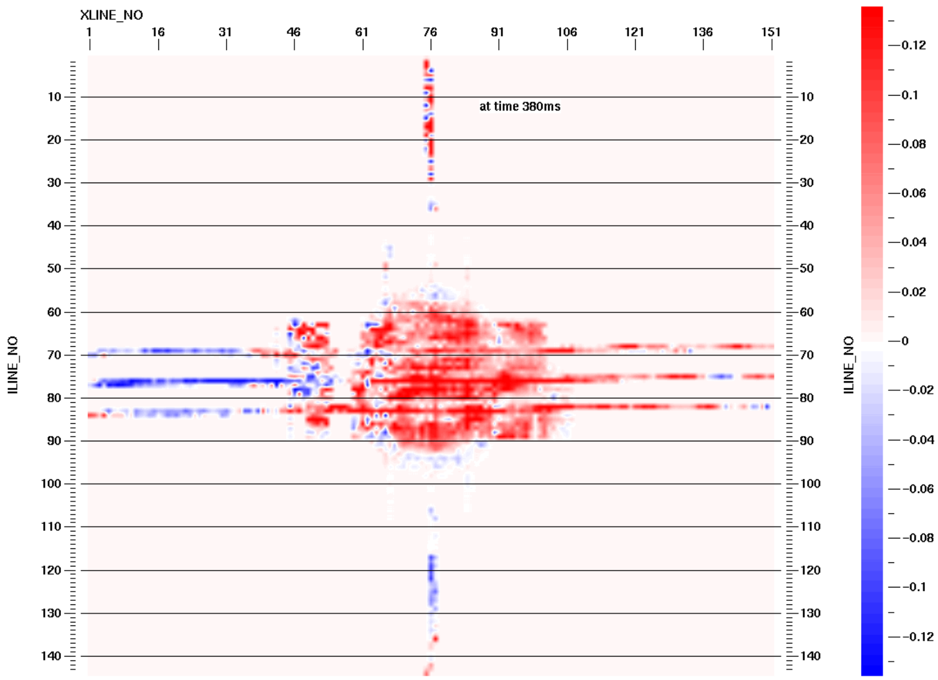
XLINE_NO
ILINE_NO
at time 380ms
0.12
0.1
0.08
0.06
0.04
0.02
0
-0.02
-0.04
-0.06
-0.08
-0.1
-0.12

b)

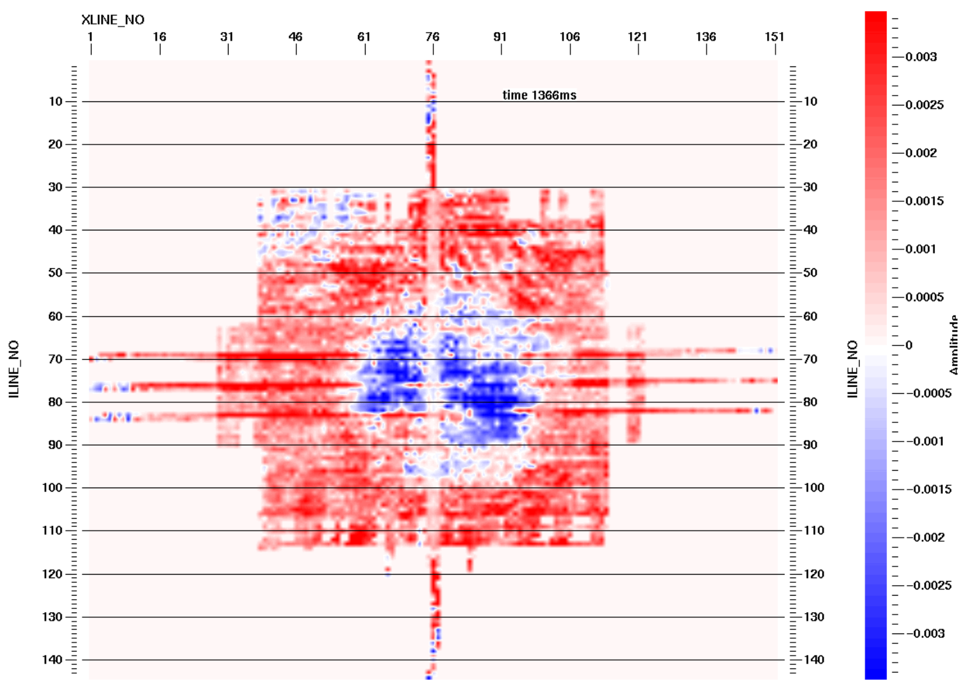
XLINE_NO
ILINE_NO
time 1366ms
0.003
0.0025
0.002
0.0015
0.001
0.0005
0
-0.0005
-0.001
-0.0015
-0.002
-0.0025
-0.003

c)

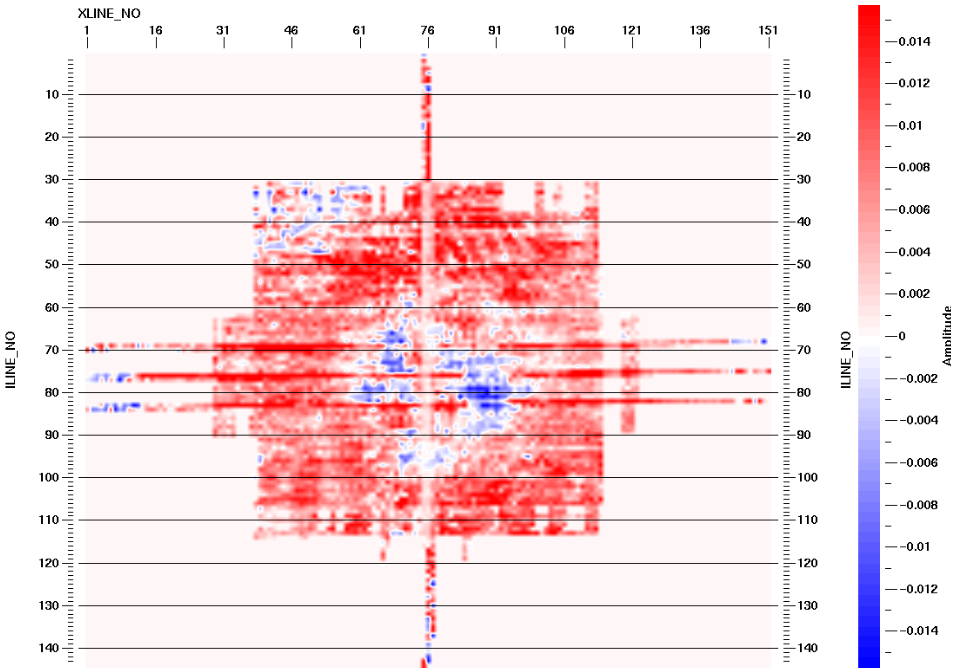

FIG. 17. Time slices from 380 ms (a), 1366 ms (b), and 1368 (c) from the 3D vertical component stack.

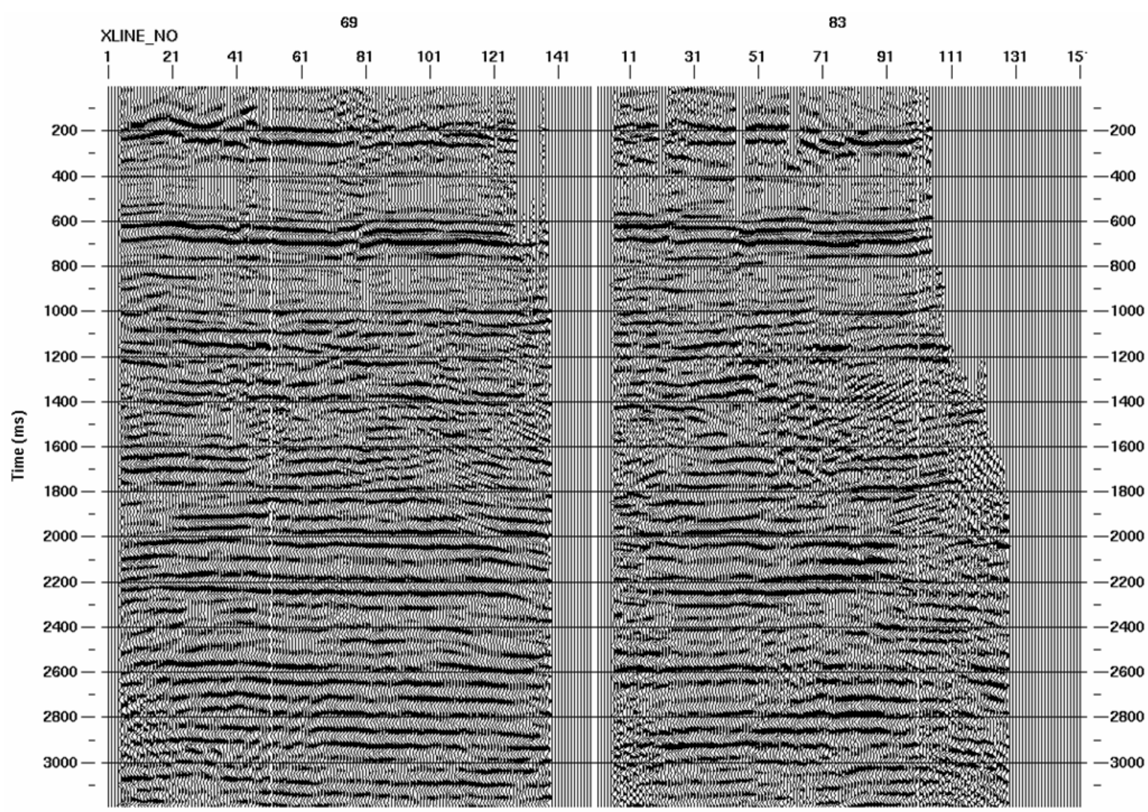

FIG. 18. Inlines 69 and 83 of the radial component 3D volume. While better than the result using P-P receiver statics (not shown), more work is clearly required.

DISCUSSION

Reprocessing of the baseline Violet Grove survey has yielded encouraging results. Data quality is high, and the vertical component processing of Line 1 is very comparable to the equivalent cross-line from the 3D volume. The process has generated a series of processing paramers and flows that will facilitate processing of the monitor survey after it is acquired in January of 2006.

ACKNOWLEDGEMENTS

The authors would like to thank AERI (Alberta Energy Research Institute), WED (Western Economic Development), Penn West Petroleum Ltd., NSERC (Natural Sciences and Engineering Research Council of Canada) and all CREWES sponsors. We would also like to thank Dr. Rolf Maier and other colleagues for their help and support. Finally, we would like to thank Landmark Graphics and Hampson Russell for the use of donated software.

REFERENCES

Chen, F., Lawton, D. C., 2005, Interpretation of baseline surface seismic data at the Violet Grove CO2 injection site, Alberta: CREWES Research Report, **17**.

Couëslan, M. L., Lawton, D. C., Jones, M., 2005, Baseline 3D VSP Survey Processing for the Violet Grove CO2 Injection Site: CREWES Research Report, **17**.

Lawton, D. C., Couëslan, M. L., Chen, F., Bland, H. C., Jones, M., Gallant, E. V., Bertram, M. B., 2005, Overview of the Violet Grove CO2 injection monitoring project: CREWES Research Report, **17**.

Lu, H., and Hall, K. W., Tutorial: Converted-wave (2D PS) processing: CREWES Research Report, **15**.

Lu, H., and Margrave, G. F., Reprocessing the Blackfoot 3C-3D seismic data: CREWES Research Report, **10**.